Full Length Research Paper

Comparison of electron transport properties in submicrometer ZnS and ZnO n+nn+ diode using ensemble Monte Carlo simulation

M. R. Khalvati[1]*, H. Arabshahi[2], M. Izadifard[1], A. Mokhles Gerami[3] and H. Rahimpour Soleimani[3]

[1]Department of Physics, Shahrood University of Technology, Shahrood, Iran.
[2]Department of Physics, Ferdowsi University of Mashhad, Mashhad, Iran.
[3]Department of Physics, University of Guilan, Rasht, Iran.

An ensemble Monte Carlo simulation has been used for the simultaneous evaluation of the electronic steady-state transport in n+nn+ ZnS and ZnO diode. The anode voltage ranges from 0 to 4 V. Electronic states within the conduction band valleys are based on a three-valley model which are represented by nonparabolic ellipsoidal valleys centered on the important symmetry point of the first Brillouin zone. Our calculation shows that the saturation mean drift velocity for electrons in the channel of ZnO and ZnS are about 2×10^5 and 1.25×10^5 ms^{-1}, respectively at a bias voltage of 4 V. It is shown also that the mean drift velocity in channel decrease sharply with increasing temperature in both structure and reach to saturated value about 1×10^5 and 0.6×10^5 ms^{-1} for ZnO and ZnS, respectively.

INTRODUCTION

The interest to study electron transport in semiconductor devices at very high electric field has been increased in the last decades (Albrecht et al., 1998). The submicrometer structure is one of the most favored devices in the construction of large scale integrated circuits because of its simplicity of construction (Brennan et al., 2002), the comparative lack of doping diffusion problems and the resultant high packing densities possible (O'Leary et al., 2006).

Non-equilibrium electron transport aspect in small semiconductor devices have arisen many efforts to improve efficiency of methods that, by solving the Boltzmman transport equation (BTE), deal with the problem of carrier transport at a microscopic level (Bhapkar et al., 1997). The drift diffusion model is not accurate enough to simulate submicrometers semiconductor devices, because it assumes a thermal equilibrium of mean carrier energy (Farahmand et al., 2001; Brennan, 1998). The approaches based on the hydrodynamic and energy transport balance can not give a self consistent description of the carrier transport (Fischetti et al., 1991). The microscopic model based on the Monte Carlo method to solve BTE seems to the most adequate for complete study of submicrometers devices (Izuka, 1990; Meinerzhagen et al., 1988).

The transport properties of ZnS and ZnO have been a subject of extensive investigation in recent years (Sandbom et al., 1989). Currently these materials are used in many electronic and optoelectronic applications such as light emitting diodes (LED's), laser systems and hetero-junction solar cells, gas sensors and MEMS (Tang et al., 1989; Kavasoglu et al., 2008).

There has been a great interest in the study of charge carrier transport of ZnS and ZnO due to the wide band gap, which has become one of the most applied semiconductors in the fabrication of electronic devices. Most of the previous theoretical work has been carried out on bulk transport properties of ZnS and ZnO (Öztas et al., 2008) and there is no significant research have been reported on electron transport characteristic in ZnS and ZnO n+nn+ (Gomeza et al., 2005). We investigate effect of applied voltage and temperature upon electron transport in ZnS and ZnO n+nn+ diodes (Han et al.,

---
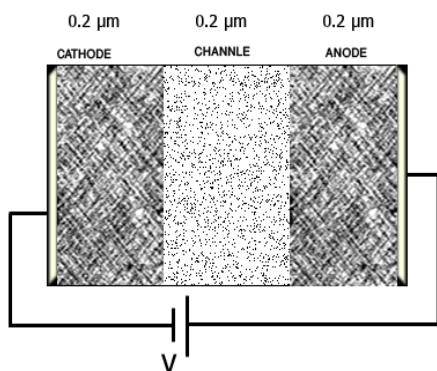*Corresponding author. E-mail: mohammad_khalvati@yahoo.com.

Figure 1. Geometry of n⁺nn⁺ diode.

Table 1. Important band parameters used in our simulation for ZnS and ZnO.

	Valley	Egap(eV)	m^*	Nonparabolicity (eV⁻¹)
	Γ	3.4	0.17	0.66
ZnO	U	7.8	0.42	0.15
	K	8.0	0.70	0.0
	Γ	3.60	0.28	0.69
ZnS	U	5.04	0.22	0.65
	K	5.05	0.64	0.36

Table 2. Material parameter selections for ZnS and ZnO.

	ZnO	ZnS
Density ρ(kgm⁻³)	5670	4070
Longitudinal sound velocity vs(ms⁻¹)	2200	5200
Low-frequency dielectric constant ε_0	8.2	8.32
High-frequency dielectric constant ε_∞	3.7	5.13
Acoustic deformation potential D(eV)	3.1	8.3
Polar optical phonon energy (eV)	0.05	0.04
Intervalley deformation potentials (10⁷ eVm⁻¹)	1	1

2009). In this paper we present simulation results for ZnS and ZnO n+nn+ diodes. The effects of bias voltage and temperature on electron drift velocity have been determined. The paper is organized as follows. The theoretical model is briefly surveyed in section 2. The application of the method to the case of ZnS and ZnO n+nn+ diodes are presented and discussed at in section 3. Some concluding remarks are reported in section 4.

Simulation models

Monte Carlo simulation has proved to be a powerful technique in electron transport in semiconductor devices. This model is based on the knowledge of the crystal structure and band structure parameters (Moglestue, 1993; Jacoboni, 1983). In our Monte Carlo models over 10⁵ quasi particles spread out into more than a hundred meshes along device length. Dirichlet boundary condition has been taken into account and results are presented for steady-state of electron transport. The n⁺nn⁺ diodes has an active n-layers with a 0.2 μm length which is sandwiched between a 0.2 μm cathode and anode n⁺-layers that are abruptly are doped to 5 × 10¹⁷ cm⁻³. Schematic view of devices has shown in Figure 1.

Details of the workings of the Monte Carlo simulator have been exhaustively presented elsewhere (Arabshahi et al., 2008) and will not be repeated here; only the main features and relevant differences will be discussed. In order to calculate the electron drift velocity for large electric fields, consideration of conduction band satellite valleys is necessary. Here the Γ valley, the six equivalent U valleys and the three equivalent K valleys for wurtzite ZnO and ZnS were represented by spherical, non-parabolic, ellipsoidal valleys expressions by the following form,

$$\varepsilon(1+\alpha\varepsilon) = \frac{\hbar^2 k^2}{2m^*} \tag{1}$$

where m^* is the effective masses and α is the nonparabolicity factors (Weng et al., 2003).

The Monte Carlo model includes polar optical, acoustic phonon, ionized impurity and non-polar intervalley phonon scattering which are the most important mechanism that can affect on the electron transport properties. The electron-electron scattering is negligible because we worked with the low doped semiconductors.

Self-consistently potential profiles have included by solving Poisson equation with the following form,

$$\nabla^2 \varphi = \frac{\rho}{\varepsilon} \tag{2}$$

This equation was solved with consideration of electron transport in a large number period of time with appropriate boundary conditions. For one dimensional case we have,

$$\frac{\varphi_{i-1} - 2\varphi_i - \varphi_{i+1}}{\Delta x^2} = -\frac{\rho_i}{\varepsilon} \tag{3}$$

where φ_i is the value of potential on each mesh and Δx^2 is the spatial mesh size[21]. The Ohmic boundary is assumed at the ends of diode with maintaining charge neutrality near each contact. The band structure and material parameters necessary for calculating the scattering probabilities used in the present Monte Carlo simulation are given in Tables 1 and 2.
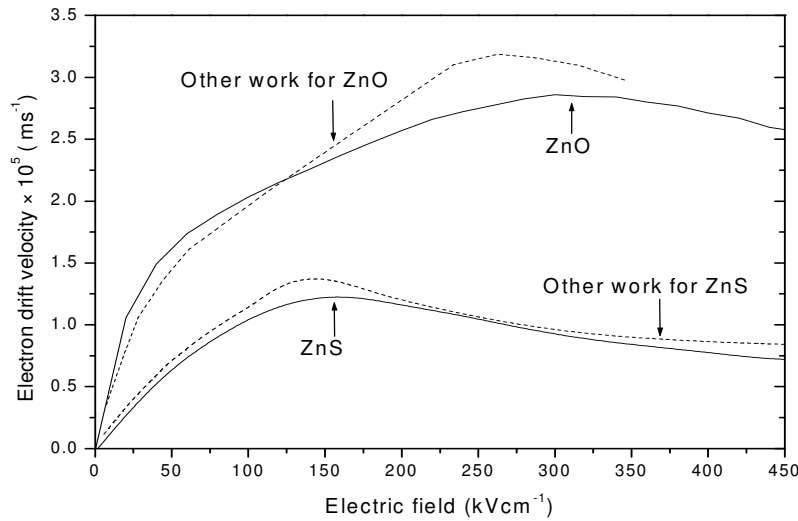
Figure 2. Electron drift velocity obtained my Monte Carlo calculation in bulk ZnO and ZnS at 300 K.
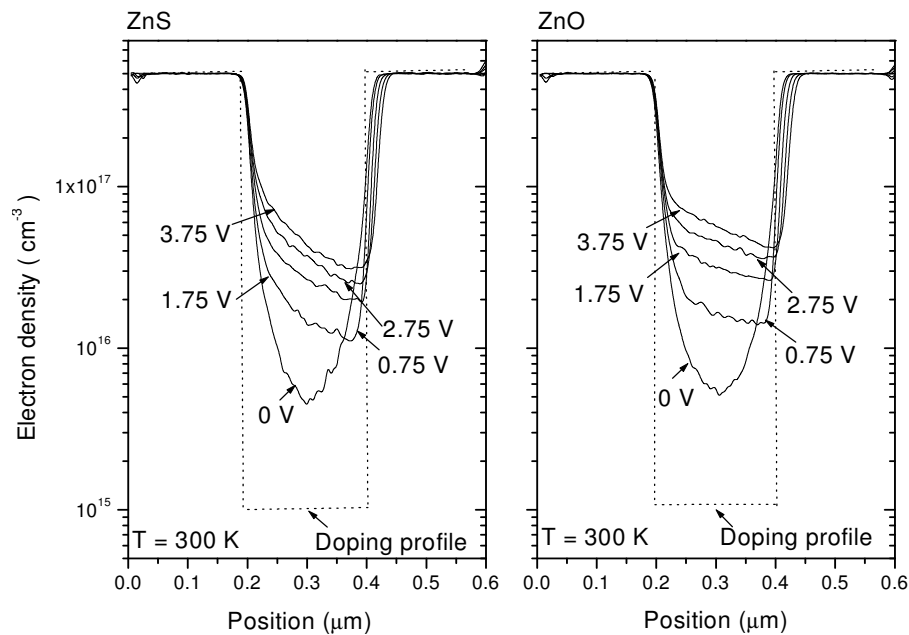

Figure 3. The distribution of the electron density along ZnO and ZnS n+nn+ diode are plotted under different bias voltages of 0, 0.75, 1.75, 2.75, 3.75 V.

RESULTS AND DISCUSSION

Before applying our transport model to the simulation of ZnS and ZnO n+nn+ diodes, and in order to check its validity, we have carried out study of electron transport in bulk of these materials under a uniform applied electric field overall bulk. Such a study allows us to found deeper inside of electron behavior in n^+nn^+ diodes. Figure 2 shows average electron drift velocity as a function of applied electric field in the room temperature. Both of

ZnS and ZnO exhibit a peak of drift velocity curves about 150 and 300 kV/cm, respectively. After these thresholds fields, velocity curves decrease slightly and finally it saturate. Dashed and doted line reported by other authors for ZnS and ZnO, respectively, which is in fair agreement with our calculated results.

Figure 3 show the free electron density as function of device length in bias voltages of 0 and 4 V for ZnS and ZnO n^+nn^+, respectively. Dashed lines demonstrate doping profile of device. It is apparently from the Figure
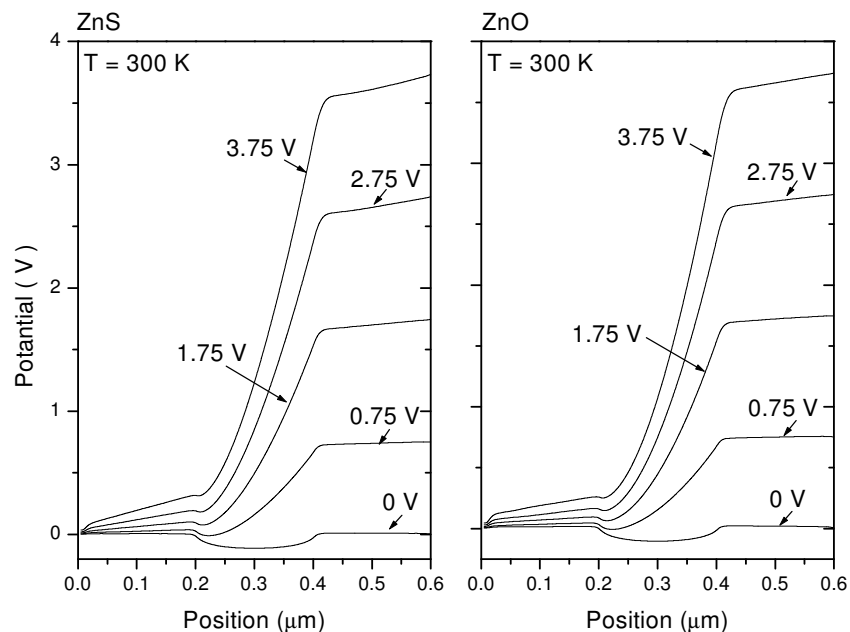
Figure 4. The distribution of the electrical potential along ZnO and ZnS n+nn+ diode are plotted under different bias voltages of 0, 0.75, 1.75, 2.75, 3.75 V.
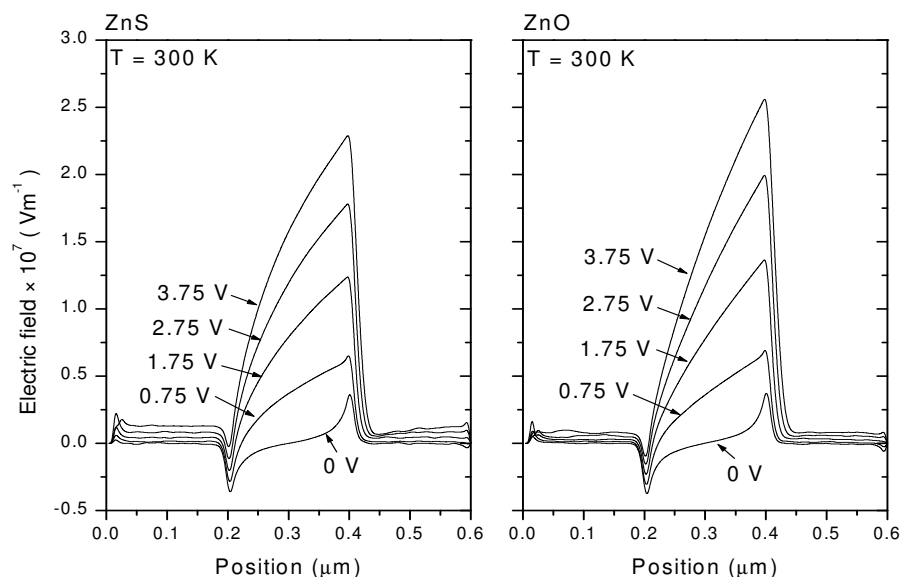

Figure 5. The distribution of the electric field along ZnO and ZnS n+nn+ diode are plotted under different bias voltages of 0, 0.75, 1.75, 2.75, 3.75 V.

that in absence of any external voltage, electrons diffuse from the n^+ region into the channel. Diffusing of electrons is due to uniform doping profile along device length. This causes a dipole of charge at the two surface of each heterojunction which induces a field opposite to the diffusion of electrons from n+ region to the channel. When a voltage is applied to contacts, electrons are injected to the channel by anode and cathode; therefore

the density of electron rises to its primitive value in this region. The electron density behavior in the channel leads to create a non-uniform potential profile and consequently electric field inside the channel[24] as it shown in Figures 4 and 5, respectively. As we expect from Figure 2, potential have slightly decrease at first homojunctions, then it increase steeply until reach to a value of applied voltage near the second hemojunctions.
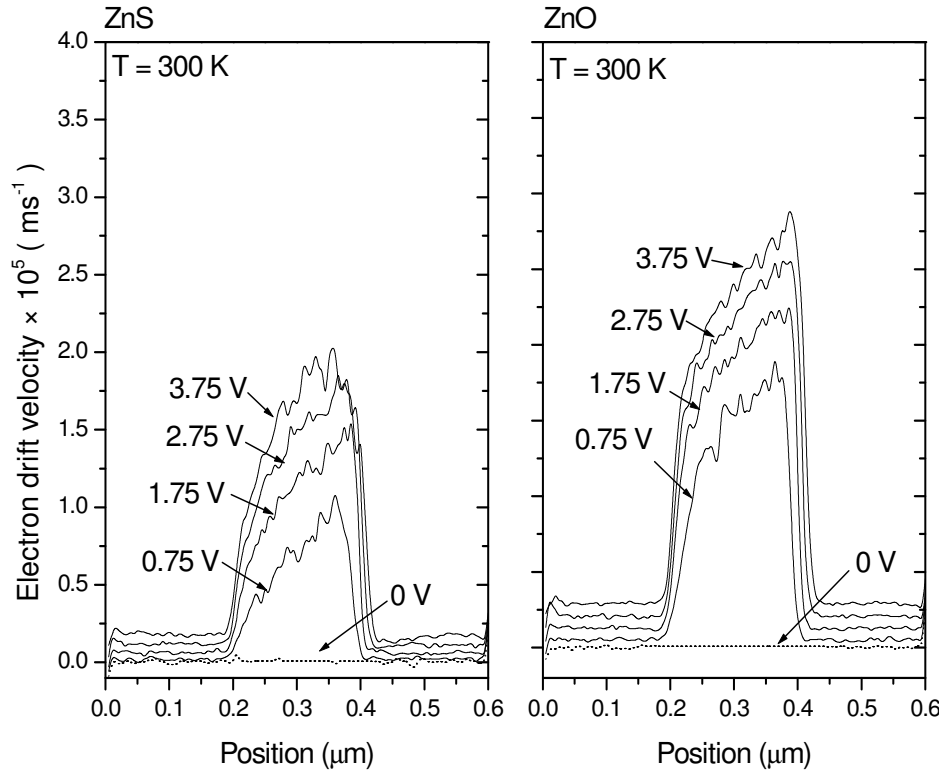
Figure 6. The distribution of the electron velocity along ZnO and ZnS n+nn+ diode are plotted under different bias voltages of 0, 0.75, 1.75, 2.75, 3.75 V.

Electric field inside the devices is obtained by calculation of distinguish of the potential inside the devices. Also with increasing the applied voltage, higher electric field can be created inside the channel, since the electric field in almost all of the channel region is an accelerating field that provides a favorable transport condition for electrons.

In Figure 6 electron drift velocity as function of applied voltage was reported at different voltages in both ZnS and ZnO n^+nn^+ diode. With increasing applied voltage, electron velocity increase inside the channel. The electrons mobility in ZnO diode is more than ZnS in the same voltage. It is partly due to heavy effective electron mass in ZnO in comparison to ZnS. Another effect that leads to exceed in velocity profile in ZnO diode is due to larger electric field in the channel region as it can be seen from Figure 5.

In Figure 7 the mean electron velocity, which were evaluated by taking an average of the velocities of all the electrons in the channel region are presented for different applied voltages. With increasing applied voltage from 0V to 4 V, mean velocity in channel have a great variation at first and for voltages above 2V mean velocity increasing slightly and for higher voltage it reach to saturation value, for example, in ZnS n+nn+ diode, the mean velocity have increase about 0.7×10^5 ms^{-1} by increasing voltage from 0 to 0.75 V but it have changed about 0.18×10^5 ms^{-1} by increasing voltage from 3 to 3.75 V. Also it is apparently

seen that electron gain more mean velocity in ZnO diode than ZnS for all voltages.

Finally Figure 7 shows the calculated mean drift velocity of electrons as a function of temperature at a constant bias voltage 3 V. As it can be seen, with increasing temperature from 300 K, the mean drift velocity for both diodes is decreased. This is due to general increasing of total scattering with temperature, which suppresses the electron energy.

CONCLUSIONS

Electron transport in ZnO and ZnS n+nn+ diodes have been simulated at different bias voltages and temperatures, using an ensemble Monte Carlo simulation. Our theoretical model includes a 2D Monte Carlo transport kernal which is coupled to a 1D poisson solver. we find that the mean electron velocity is always more in ZnO n+nn+ diode at all of voltages range from 0 to 4 V and finally it reaches to a value about 2.0×10^5 and 1.25×10^5 ms^{-1} for ZnO and ZnS, respectively.

ACKNOWLEDEGMENT

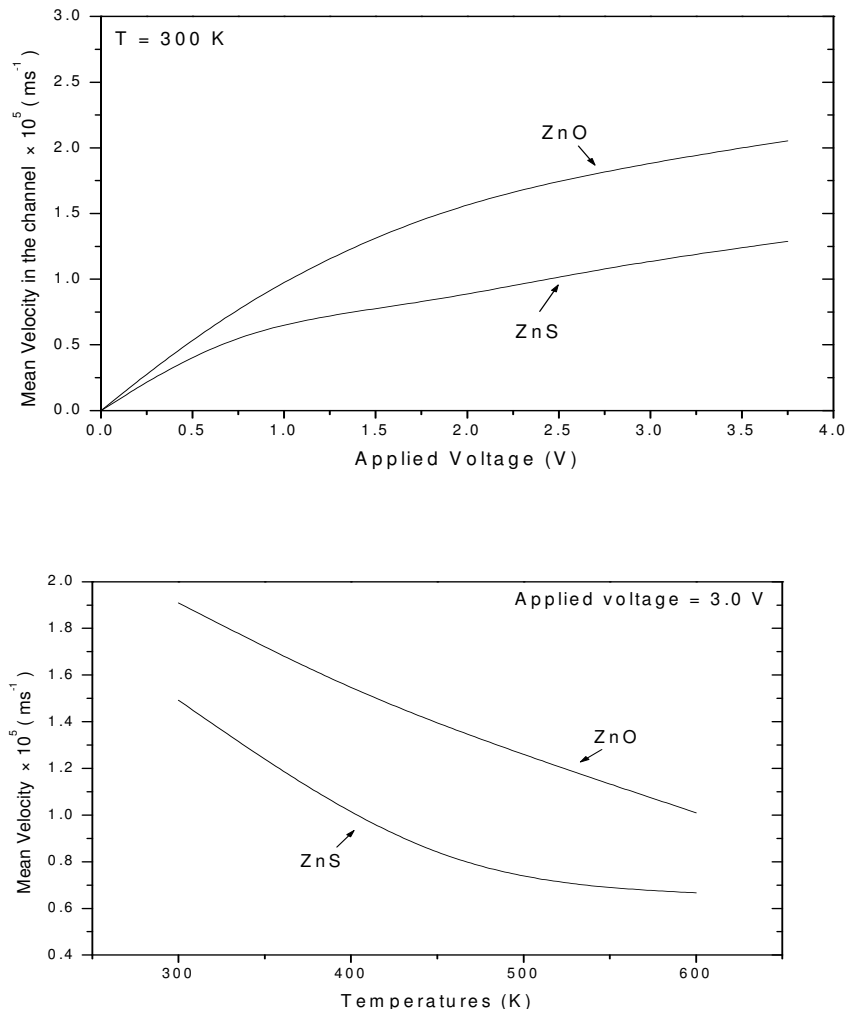I would like to thank Maryam Gholvani Naeeini for her

Figure 7. The mean electrons drift velocity as function of applied voltage in ZnO and ZnS diode.

useful comments and writing up the paper.

REFERENCES

Albrecht JD, Wang RP, Ruden PP, Farahmand M, Brennan KF (1998). Electron transport characteristics of GaN for high temperature device modeling, J. Appl. Phys., 83: 4777-4781.

Arabshahi H, Khalvati MR, Rezaee R, Abadi M (2008). *Comparisonof* steady-state and transient electron transport in InAs, InP AND GaAs, Modern Phys. Lett. B, 22(17): 1695-1702.

Arabshahi H, Khalvati MR, Rezaee R, Abadi M (2008). Temperature and Doping Dependencies of Electron Mobility in InAs,AlAs and AlGaAs at High Electric Field Application, Brazilian J. Phys., 38(3A): 293-296.

Bhapkar UV, Shur MS (1997). Monte Carlo calculation of velocity-field characteristics of wurtzite GaN, J. Appl. Phys., 82: 1649-1655.

Brennan KF, Belloti E, Farahmand M, Haralson J, Ruden PP, Albrecht JD, Sutandi A (2000). Materials theory based modeling of wide band gap semiconductors: From basic properties to devices, Solid-State electronics, 44: 195-204.

Brennan KF, Brown AS (2002). Theory of modern electronic semiconductor devices, John Wiley & Sons, Inc.

Brennan KF (1998) Theory of high-field electronic transport in bulk ZnS and ZnSe, J. Appl. Phys., 64: 4024-4030.

Farahmand M, Goano M, Ruden PP (2001). Monte Carlo Simulation of Electron Transport in the III-Nitride Wurtzite Phase Materials System: Binaries and Ternaries, IEEE trans. electron devices, 48(3): 535-542.

Fischetti MV, Laux SE (1991). Monte Carlo Simulation of Transport in Technologically Significant Semiconductors of the Diamond and Zinc-Blende Structures-Part 11: Submicrometer MOSFET's, IEEE Trans. Electron Devices, 38: 650-660.

Jacoboni C, Lugli P (1989). The monte carlo method for semiconductor device simulation, springer–Verlag.

Izuka T, Fukuma M (1990). Camer transport simulator for silicon based on camer distribution function evolution, Solid-State Electron, 33, 27-34.

Kavasoglu N, Kavasoglu AS (2008) Admittance spectroscopy of spray-pyrolyzed ZnO film, Physica B, 403: 3159-3163.

Gomez H, Maldonado A, Olvera M. de la L, Acosta DR (2005) Gallium-doped ZnO thin films deposited by chemical spray, Solar Energy Mater. Solar Cells, 87: 107-116.

Han N, Tian Y, Wu X, Chen Y (2009) Improving humidity selectivity in formaldehyde gas sensing by a two-sensor array made of Ga-doped ZnO, Sensors and Actuators B, 138: 228-235.

Meinerzhagen B, Engl WL (1988) The Influence of the Thermal Equilibrium Approximation on the Accuracy Classical Two-Dimensional Numerical Modeling of Silicon Submicrometer MOS Transistors, IEEE Trans. Electron Devices, 35: 689-697.

Moglestue M (1993) Monte Carlo simulation of semiconductor devices, chapman & Hall.

O'Leary SK, Foutz BE, Shur MS, Eastman LF (2006) Potential performance of indium-nitride-based devices, Appl. Phys. Lett., 88: 152113.

Öztas M, Bedir B (2008) Thickness dependence of structural, electrical and optical properties of sprayed ZnO:Cu films, Thin Solid Films, 516: 1703-1709.

Sandborn PA, Rao A, Blakey PA (1989) An assessment of approximate nonstationary charge transport models used for GaAs device modeling, IEEE Trans. Electron Devices, 36(7): 1244-1253.